

REPORT DOCUMENTATION PAGE				Form Approved OMB No. 0704-0188	
Public reporting burden for this collection of information is estimated to average 1 hour per response, including the time for reviewing instructions, searching existing data sources, gathering and maintaining the data needed, and completing and reviewing this collection of information. Send comments regarding this burden estimate or any other aspect of this collection of information, including suggestions for reducing this burden to Department of Defense, Washington Headquarters Services, Directorate for Information Operations and Reports (0704-0188), 1215 Jefferson Davis Highway, Suite 1204, Arlington, VA 22202-4302. Respondents should be aware that notwithstanding any other provision of law, no person shall be subject to any penalty for failing to comply with a collection of information if it does not display a currently valid OMB control number. PLEASE DO NOT RETURN YOUR FORM TO THE ABOVE ADDRESS.					
1. REPORT DATE (DD-MM-YYYY) 30-06-2008		2. REPORT TYPE Technical Paper		3. DATES COVERED (From - To)	
4. TITLE AND SUBTITLE Thermal Stability and Heat Transfer Characteristics of RP-2 (Preprint)				5a. CONTRACT NUMBER	
				5b. GRANT NUMBER	
				5c. PROGRAM ELEMENT NUMBER	
6. AUTHOR(S) Matthew Billingsley (AFRL/RZSA)				5d. PROJECT NUMBER	
				5e. TASK NUMBER 48470244	
				5f. WORK UNIT NUMBER	
7. PERFORMING ORGANIZATION NAME(S) AND ADDRESS(ES) Air Force Research Laboratory (AFMC) AFRL/RZSA 10 E. Saturn Blvd. Edwards AFB CA 93524-7680				8. PERFORMING ORGANIZATION REPORT NUMBER AFRL-RZ-ED-TP-2008-259	
9. SPONSORING / MONITORING AGENCY NAME(S) AND ADDRESS(ES) Air Force Research Laboratory (AFMC) AFRL/RZS 5 Pollux Drive Edwards AFB CA 93524-7048				10. SPONSOR/MONITOR'S ACRONYM(S)	
				11. SPONSOR/MONITOR'S NUMBER(S) AFRL-RZ-ED-TP-2008-259	
12. DISTRIBUTION / AVAILABILITY STATEMENT Approved for public release; distribution unlimited (PA #08259A).					
13. SUPPLEMENTARY NOTES For presentation at the 44 th AIAA Joint Propulsion Conference, Hartford, CT, 20-23 July 2008.					
14. ABSTRACT In an effort to enable reusable, high-performing liquid rocket engines, a comprehensive experimental and numerical investigation of the thermal performance (thermal stability and heat transfer characteristics) of RP-2 is underway at the Air Force Research Laboratory (AFRL), Edwards AFB, CA. In the current work, the High Heat Flux Facility (HHFF) was used to provide initial RP-2 thermal performance information under conditions simulative of those encountered in the cooling channels of a real engine. RP-2 was thermally stressed while flowing through circular copper tube test sections. Short-duration thermal stressing tests provided heat transfer information which closely followed existing empirical correlations for RP-1. Effects of wall temperature, bulk temperature, and flow rate on heat transfer were observed and were consistent with expected behavior. Longer-duration tests at elevated wall temperatures provided the first steps in elucidating the conditions under which solid carbon deposits form. The test sections were analyzed post-test with optical and scanning electron microscope and carbon deposition burn-off for signs of coke formation. The results from these analyses indicate the presence of solid carbon deposition for high-wall temperature tests exceeding 30 min. in duration, although further testing is required to make more conclusive comparisons.					
15. SUBJECT TERMS					
16. SECURITY CLASSIFICATION OF:			17. LIMITATION OF ABSTRACT SAR	18. NUMBER OF PAGES 11	19a. NAME OF RESPONSIBLE PERSON Matthew Billingsley
a. REPORT Unclassified	b. ABSTRACT Unclassified	c. THIS PAGE Unclassified			19b. TELEPHONE NUMBER (include area code) N/A

Thermal Stability and Heat Transfer Characteristics of RP-2 (Preprint)

Matthew C. Billingsley
Air Force Research Laboratory, Edwards AFB, CA, USA

In an effort to enable reusable, high-performing liquid rocket engines, a comprehensive experimental and numerical investigation of the thermal performance (thermal stability and heat transfer characteristics) of RP-2 is underway at the Air Force Research Laboratory (AFRL), Edwards AFB, CA. In the current work, the High Heat Flux Facility (HHFF) was used to provide initial RP-2 thermal performance information under conditions simulative of those encountered in the cooling channels of a real engine. RP-2 was thermally stressed while flowing through circular copper tube test sections. Short-duration thermal stressing tests provided heat transfer information which closely followed existing empirical correlations for RP-1. Effects of wall temperature, bulk temperature, and flow rate on heat transfer were observed and were consistent with expected behavior. Longer-duration tests at elevated wall temperatures provided the first steps in elucidating the conditions under which solid carbon deposits form. The test sections were analyzed post-test with optical and scanning electron microscope and carbon deposition burn-off for signs of coke formation. The results from these analyses indicate the presence of solid carbon deposition for high-wall temperature tests exceeding 30 min. in duration, although further testing is required to make more conclusive comparisons.

I. Introduction

IMPROVED understanding and characterization of fuel thermal stability is required for the design and development of long-life, reusable liquid rocket engines. Regeneratively-cooled hydrocarbon engines maintain wall conditions below failure limits by actively cooling the thrust chamber assembly with fuel prior to fuel injection. During this process, the fuel absorbs a tremendous amount of heat and may undergo molecular decomposition, eventually resulting in insoluble products depositing on the cooling channel walls. This deposition tends to insulate the wall material, causing localized hot spots which can ultimately lead to structural failure. Thoroughly characterizing the chemical and physical processes of fuel decomposition and deposition and the conditions under which they occur will enable engine designers in the process of developing reusable, highly operable engines. Improving a fuel's ability to absorb heat without coking is also desirable from a performance standpoint. The present work is an experimental investigation of the thermal stability of the kerosene-based rocket fuel RP-2 in a heated tube under realistic fluid and thermal conditions. Thermal stability was gauged by several factors, including deposit formation and heat transfer.

Coking temperature is often referred to as the temperature above which solid deposition readily occurs, and wetted wall temperatures exceeding this limit are intentionally avoided in the design of thrust chamber assemblies. However, the chemical process of thermal decomposition and the physical process of deposit formation are influenced by several factors: fuel composition, wall roughness and material, residence time, bulk fluid conditions, and numerous temperature-dependent physical properties. The variety of contributing factors leads to a wide variability in reported coking temperatures for rocket kerosene. For RP-1 (MIL-DTL-25576E, 2006), a narrow-range kerosene fraction developed in the 1950's, reported coking wall temperature limits range from 550-850°F (561-727K). To properly quantify a fuel's thermal stability in terms of coking temperature, understanding the effects of the aforementioned influences is important.

With this in mind, AFRL's High Heat Flux Facility (HHFF), Edwards AFB, CA, was used to thermally stress RP-2 in a high-temperature, high-pressure environment. The effort discussed in this paper is part of a comprehensive program intended to develop and transition improved hydrocarbon fuels for use in liquid rocket engines. This includes full characterization of the fuel's thermal performance (thermal stability and heat transfer characteristics). A specific goal for the current work was to provide an initial measure of the thermal performance of RP-2. This was attempted by flowing fuel at relatively low velocity and high wall temperature channels and observing signs of solid deposition formation.

II. Experimental Setup and Procedures

The HHFF is a relatively new rig capable of simulating a realistic cooling channel environment and providing fuel thermal stability data over a wide variety of operating conditions. It allows for flexibility in several regards, including cooling channel geometry and material, wetted wall temperature, flow velocity, fuel composition, and channel surface features. The ability to preheat the fuel allows examination of the effect of bulk inlet temperature and comparison of core flow/boundary layer chemistry effects. A thorough discussion of the facility design is provided in Reference 1.

The current testing took advantage of flexibility in test section geometry by utilizing a simplified channel configuration. The simplified geometry was used for several reasons. First, it provided a useful comparison with existing heated tube data such as the Heated Tube Facility at NASA's Glenn Research Center² (RP-2 thermal stability testing is currently being conducted in that facility at different conditions, with comparisons forthcoming). Second, in fuel characterization work, an extensive experimental effort is necessary, and a simplified geometry is an efficient way of examining the general thermal performance, specifically fuel decomposition and its effects. When testing conditions such as wetted wall temperature and residence time are established which produce measurable levels of coke, realistic test section geometries and flow conditions are planned. Third, the test sections are relatively inexpensive and readily available.

The experimental setup for the current work is shown in Figure 1. Heat transfer from the copper heater block to the test section occurred asymmetrically across a semi-circular contact surface area formed by a groove in the heater block in which the test section fit snugly. The test section tube rested in a cradle of low-thermal conductivity ceramic, minimizing conduction to the assembly and simulating asymmetric heat transfer. In turn, the test section

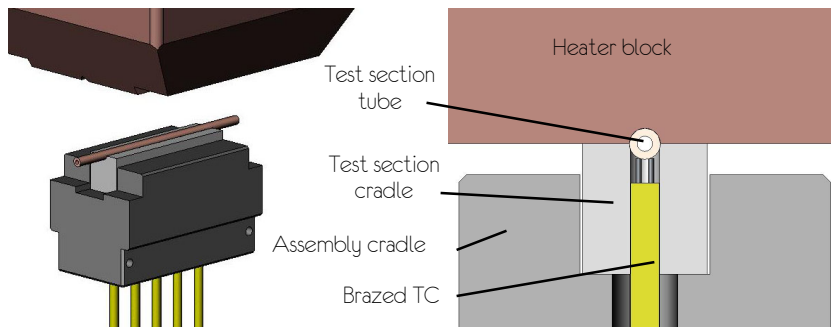


Figure 1. Experimental test section configuration. Left view shows cradle assembly and a portion of test section tube. Right view is a cutaway showing thermocouple and heater block contact with tube. Test section tube is OFE copper, 1/8-in. O.D., 0.032-in. wall thickness (nominal). Thermocouple beads are silver-soldered to test section tube.

and its cradle rested in a higher strength ceramic cradle which was supported by an aluminum fixture suspended in a vacuum chamber.

Conducting experiments under high vacuum minimized convective losses to the surroundings and oxidation on the copper surfaces. Five K-type right-angle ribbon thermocouples were brazed along the bottom centerline of each test section with 0.4-in. (10-mm) spacing. Thermocouple leads passed through holes in both ceramic cradles. One K-type spring-

loaded thermocouple measured the temperature near the bottom of the heater block during the test. The heater block temperature was maintained with twenty-five 800W custom Watlow Firerod cartridge heaters with embedded K-type thermocouples with mineral insulated leads, controlled at the console through a Watlow MLS 332 controller. Transducer data was collected at a sample rate of 100 Hz with Pacific Instruments 6013 8-channel amplifier-digitizer cards, and previewed/recorded using Pacific Instruments PI660 software.

High-pressure bladder tanks were used to pressurize the fuel, with pressure regulated by a Tescom ER3000 electronic pressure controller using a PID algorithm. A Coriolis mass flow meter measured the fuel flow rate with a stated uncertainty of $\pm 0.1\%$ at the flow rates tested. A preheater upstream of the test section was used to raise the bulk fluid temperature when desired. Cavitating venturis of varying throat area maintained constant mass flow rate despite fluctuations in downstream pressure. Most of the venturis used in the testing operate effectively at up to 75-80% pressure recovery. A backpressure control valve was used to maintain test section pressure greater than 1000 psi (48 kPa) to minimize boiling and two-phase phenomena and sharp transport property gradients near the critical point. Downstream of the test section, the fuel was collected and either reloaded or discarded, depending on the test objectives.

A typical test procedure involved increasing the fuel preheater and heater block to their specified temperatures, increasing system pressure, and adjusting the backpressure valve and pressure-regulating ER3000 to obtain the desired test section velocity and pressure. When flow conditions were reached, data recording began and the heater block was lowered onto the test section tube. An increase in the tube thermocouples occurred instantly. Flow

conditions were maintained and the heater block remained in contact with the test section tube for the duration of the test, which ranged from 2 – 40 min. for the results presented. After this time, the heater block was raised, fuel flow was stopped, and the test section was purged with low-pressure nitrogen to remove any residual fuel. The block and tube assembly then cooled under vacuum, and finally the test section was removed and prepared for analysis.

III. Results and Discussion

A. Heat Transfer Results

Several shorter-duration tests were conducted to examine the relationship between fuel bulk temperature, wetted wall temperature, and heat transfer. Minimal coke formation was expected with little influence on the measured heat transfer rates. For this reason, test sections were reused for several tests, which helped improve repeatability of thermo-fluid conditions. Surface and fluid temperature measurements were averaged over the steady-state portion of each run, usually between 2-3 min. During this time, surface temperatures varied little, but in some cases experienced an approximate 3% decrease as heat transfer occurred along the tube. Typical variation in measured surface temperature between axial locations was within 3% of the average measured temperature. This can be seen in Figure 2, showing measured surface temperatures for a representative run. The thick dashed lines indicate the user-selected portion of the test for which data were included in heat transfer calculations, and the parenthesized numbers in the legend are the axial distance

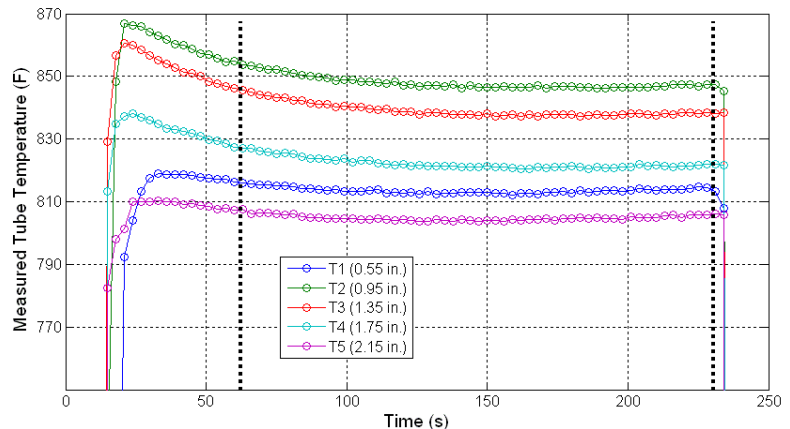


Figure 2. Measured temperature histories for a representative short-duration heat transfer test. Data used for heat transfer calculations is bounded by thick dashed lines. Thermocouple axial location is indicated in parentheses.

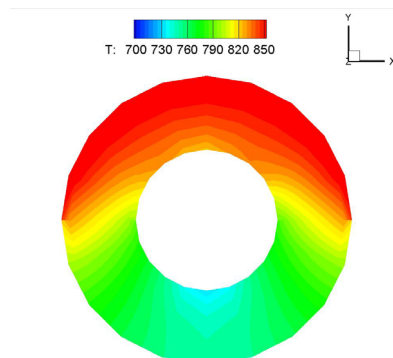


Figure 3. Temperature contours for axisymmetric heat transfer to tubular test section (scale in K). Conjugate heat transfer calculations reveal large temperature gradients around inner (wetted) wall circumference.

energy increase in the fuel was due to conduction around the circumference of the tube, a less than 3% decrease in temperature from the outer surface to the inner surface was calculated.

A more significant complication in temperature reporting arises from the circumferential variation in temperature around the inner surface of the tube. The asymmetric heat transfer results in large differences between, for example,

the upper wetted wall temperature and the lower wetted wall temperature. Conjugate heat transfer computations with Metacomp's CFD++ showed that for an 892°F (751 K) temperature measured directly at the outer bottom surface at the axial midpoint of the tube, temperature variations around the circumference of the inner fluid interface of 860-1043°F (733-835 K) were present, with an average wall temperature of 962°F (790 K). In other words, the asymmetric heat transfer results in much higher temperatures at the upper wetted surface of the tube than indicated by the lower, outside thermocouple measurements. In fact, the circumferentially-averaged wetted wall temperature in this case is 70°F (39 K) greater than the measured temperature on the lower, outer tube surface. Temperature contour results from the conjugate heat transfer calculation are given in Figure 3. Because of the marked differences, it should be noted that in reporting temperatures, the term *measured* refers to the outer, lower tube surface temperature which was measured by the thermocouple, the term *corrected* refers to the inner, average wetted wall temperature, and the term *maximum* refers to the inner, upper wetted wall temperature.

Heat transfer characteristics for the short-duration RP-2 tests are presented in Figure 4. The measured wall temperature (x-axis) is the spatially- and temporally-averaged value described above. Three data sets are shown: Set 1 data was collected with a mass flow rate (average) of 4.52 lb_m/min (0.034 kg/s) and $T_{m,i}$ of 91°F (306 K); Set 2 data was collected with a mass flow rate (average) of 3.07 lb_m/min (0.023 kg/s) and $T_{m,i}$ of 86°F (303 K); and Set 3 data was collected with a mass flow rate (average) of 4.39 lb_m/min (0.033 kg/s) and $T_{m,i}$ of 182°F (357 K). The average tube heat flux q'' (y-axis) was calculated according to the overall energy balance shown in Eq. (1). $T_{m,i}$ and $T_{m,o}$ are the measured inlet and outlet bulk fuel temperatures, respectively. Specific heat c_p was evaluated at the average bulk fluid temperature, $T_b = (T_{m,o} + T_{m,i})/2$. A_s is the surface area over which the heat transfer occurred, and \dot{m} is fuel mass flow rate.

$$q'' = \frac{\dot{m} c_p (T_{m,o} - T_{m,i})}{A_s} \quad (1)$$

One useful heat transfer result is given by Set 1 and Set 3 data, which provide a comparison showing the influence of bulk fluid temperature for similar wall temperatures and mass flow rates. For similar wall temperatures and flow rates, it is clearly seen that increasing the bulk fluid temperature by use of the preheater increases the overall heat transfer in the test section. This increase in heat transfer for higher bulk temperature fluids has been shown for aviation kerosenes previously,⁴ and is attributed to higher Reynolds numbers accompanying higher temperatures. For constant velocity and hydraulic diameter, the increase in Reynolds number between Set 1 and Set 3 is dominated by the ratio of absolute viscosities (μ_{Set1}/μ_{Set3}), leading to large Reynolds number increases for moderate temperature increases. The strong dependence of convective heat transfer coefficient on bulk temperature

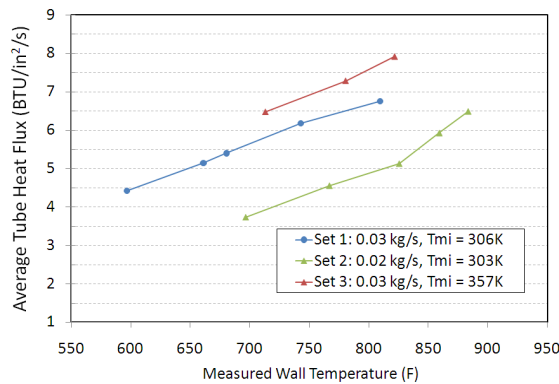


Figure 4. Average tube heat flux as a function of wall temperature for short duration tests in copper tube at varying flow conditions. For similar wall temperature and bulk inlet temperature, Set 2 heat flux is less than Set 1 heat flux due to a lower mass flow rate. Heat transfer for Set 3 is greater than that for Set 1 due to higher inlet bulk fuel temperature, with similar mass flow rate and wall temperature.

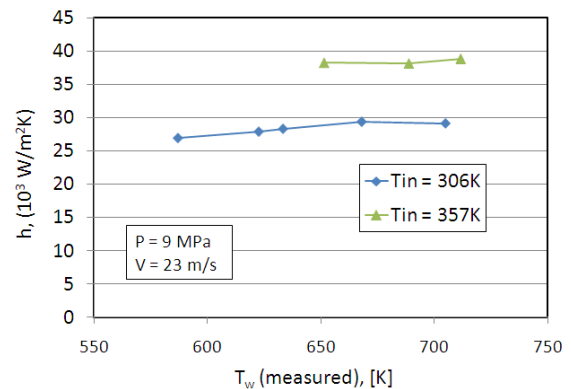


Figure 5. Dependence of average convective heat transfer coefficient on bulk fluid temperature. Moderate increases in bulk temperature cause significant enhancement of average heat transfer coefficient for runs with similar mass flow rate and wall temperature. Average convective heat transfer coefficient between runs is not a strong function of wall temperature.

is presented in Figure 5, reproduced in a similar format as provided in Reference 4 for direct comparison. In this case, an increase in bulk temperature of about 17% causes an increase in average convective heat transfer coefficient of about 36%.

The data of Set 1 and Set 2 provide a comparison showing the influence of mass flow rate on heat transfer for similar wall and bulk fluid temperatures. As expected according to Eq. (1), Set 1 has correspondingly greater heat transfer by a factor nearly identical to the increase in mass flow rate. Finally, for all data, increasing wall temperature is accompanied by an expected increase in heat transfer rate.

To accurately predict and correlate heat transfer results, fluid thermophysical property data over a wide range of temperatures and pressures is necessary. Currently, the Physical and Chemical Properties Division of the National Institute of Standards and Technology (NIST) is compiling high-accuracy thermophysical property data of rocket propellants RP-1 and RP-2. At the time of writing, those results were not available. However, the comparison between RP-2 and RP-1 properties at lower temperatures is in close agreement. Therefore, RP-1 properties at elevated temperatures were accepted as representative of RP-2.

Figure 6 compares nondimensionalized heat transfer data with two correlations from previous hydrocarbon thermal stability research.² In that work, multiple linear regressions were performed to fit heat transfer data for a variety of hydrocarbon fuels, resulting in fuel-specific constants. These correlations account for entrance effects with the term $1+2/(x/d)$, where x is the tube length and d is the inner diameter, but do not factor in viscosity variations between the bulk fluid and the fluid at the wall. The current data is compared with correlation curve-fits

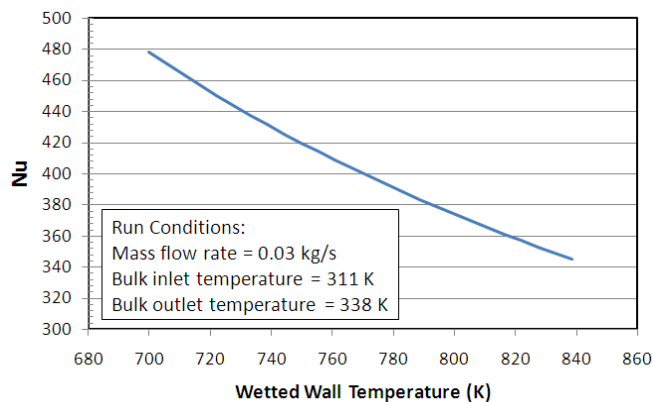


Figure 7. Influence of wall temperature on heat transfer for a given set of run conditions. For higher wall temperatures, a lower heat transfer coefficient is required to cause a given increase in bulk fuel temperature. This effect caused a downward shift in Nu when correcting for the actual wetted wall temperature.

for co-mingled fuel (solid line) and RP-1 (dashed line). First, the data are presented without error bars to indicate the conditions (velocity and bulk inlet temperature) under which they occurred. For example, higher Reynolds numbers in this case were gained not by increasing the velocity, but by decreasing the viscosity through preheating. The data are reproduced as “Corrected Data,” with $\pm 10\%$ error bars reflecting the uncertainties in physical property data: thermal conductivity k , specific heat c_p , absolute viscosity μ , and density ρ . The data with error bars have been corrected for the variation in measured and actual wall temperature so that a decrease in Nu occurs. The measured increase in fuel temperature actually took place under slightly hotter average temperatures, so heat transfer for the uncorrected data was overestimated. The influence of wall temperature on heat transfer for a given bulk temperature increase (that is,

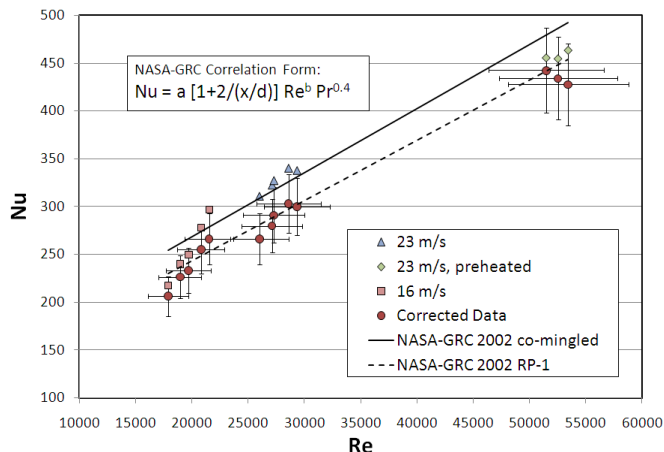


Figure 6. Nondimensional heat transfer results compared with NASA-GRC heated tube facility correlations. Good agreement is seen between the current data and existing heat transfer correlations. Correlation constants: for co-mingled fuels, $a = 0.016$, $b = 0.862$; for RP-1, $a = 0.012$, $b = 0.879$.

for a given run) is shown in Figure 7. The run conditions are noted in the figure. In words, the figure says that achieving a given increase in bulk fuel temperature requires a higher convective heat transfer coefficient for lower wall temperatures than for higher wall temperatures, which is somewhat intuitive, and is the reason for the shift down in the corrected data of Figure 6. It is also noteworthy to consider the relative impact that inaccurate surface temperature measurements and/or temperature corrections may have on heat transfer results. As shown, correcting

for the actual wall temperature causes the data to correspond well with the RP-1 correlation of NASA-GRC. In general, heat transfer data is in good overall agreement with results from previous research.

B. Visible Deposit Formation

Previous research involving RP-1 coking indicated that relatively long test durations are required to produce a measureable amount of carbon deposit on the wetted surface.^{2,5} It is expected that RP-2, with significantly lower sulfur content, will require even longer thermal stressing periods to produce a comparable amount of deposit as was measured for the RP-1 testing. In addition to time duration of thermal stressing, deposition is affected by surface temperature. In an attempt to study the time and temperature conditions at which coke deposit forms for RP-2, a significant portion of the current work comprised relatively long duration thermal stressing periods at average measured wall temperatures expected to produce measurable levels of solid deposit. The average fuel inlet temperature was adjusted by utilizing the preheater prior to the fuel entering the test section. The test duration approached the system capability for the flow rates tested. New channel sections were used for each test to provide side-by-side comparison of known condition tests.

Following each test, the test sections were prepared for visual examination and carbon deposition measurements. The test handling procedure involved removing the braze material from the outside of the tube, measuring, marking, and cutting the tubes, rinsing the sections to remove any residual hydrocarbons, and vacuum-drying to remove the solvent. Figure 8 shows the locations of the thermocouple measurements with respect to the heated portion and the locations where the tube was cut. Three 1-in. segments of each 8-in. tube were kept for visual inspection. To examine the inner surface, a 6mm-dia. end mill was used to cut through the tube, exposing the upper, wetted wall of the tube.

Qualitative observation is a simple yet useful way to obtain decomposition and/or coking information following a thermal stressing test. Fuel samples were drawn from the collection tank after each test and stored in clear vials. Visual comparison of these samples with unstressed fuel showed no noticeable discoloration or suspended

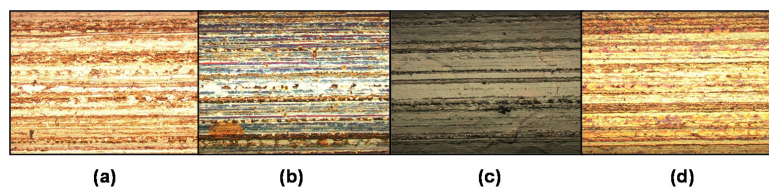


Figure 9. Optical microscope images of RP-2 thermal stressing tests in copper tube test sections. A blank segment (a) is provided for comparison of deposit formation with the inlet (b), middle (c), and outlet (d) test section segments. Varying degree of discoloration occurred, with the middle segment having a layer deposit buildup. The corresponding test used preheated fuel at a high wall temperature and long thermal stressing duration. Magnification is approximately 200x.

particulates, which have been reported as measures of significant decomposition in previous testing with aviation hydrocarbons.^{6,7} The lack of turbidity is not surprising, as the fraction of fuel exposed to the hot wall was limited to the thermal boundary layer in the test section.

Visual inspection of the test sections provided quick information on the presence of coke formation. A Nikon MM-400 optical microscope was used to give initial indication of deposit morphology. The microscope's objective head was

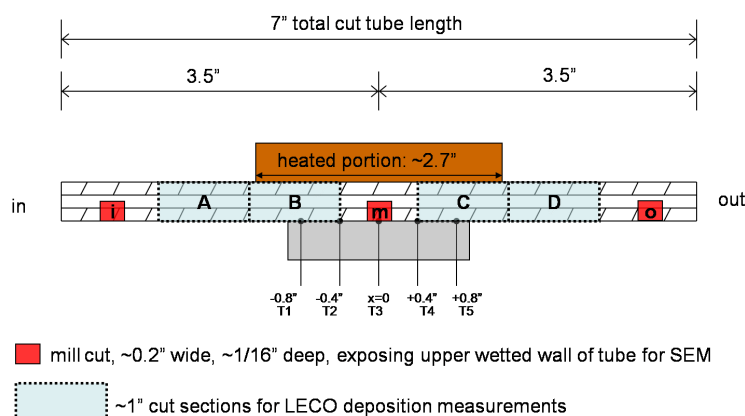


Figure 8. Test section analysis geometry. Each test section for the long-duration thermal stability tests was cut as shown above. Note that the 1-in. sections A and D occur outside the heat transfer portion of the tube.

automatically incremented in the z-direction (up-down) to provide a series of focused images which were then superimposed to produce a focused, magnified image of the test section surface. A comparison of these images for segments i, m, and o (see Figure 8), along with an unused segment are given in Figure 9. Exposure was maintained constant to allow comparison. The bright horizontal band seen across the middle of the segments is due to reflection

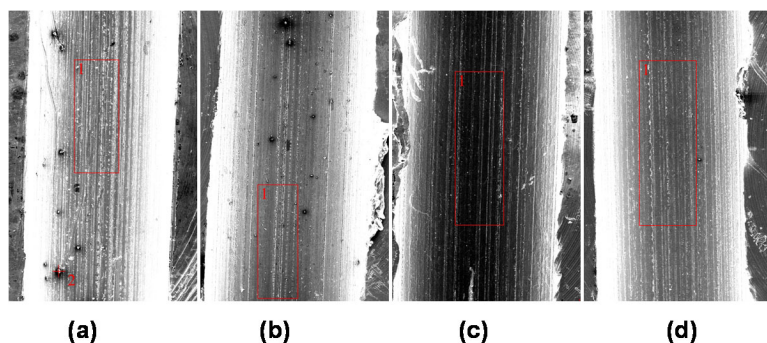


Figure 10. Scanning electron microscope images of RP-2 thermal stressing tests in copper tube section. SEM images were used as an indicator of surface deposit features for blank segment (a)(38x), inlet (b)(43x), middle (c)(44x), and outlet (d)(44x). The corresponding test section used preheated fuel at a high wall temperature and long thermal stressing duration. Dark spots on segment (b) could be onset of deposition or surface contaminants. Limited deposition features are visible on segment (c). Surface striations on (d) appear more pronounced than (b).

In addition to the optical images, magnified details of deposit formation features were obtained with an FEI Quanta 600 Scanning electron microscope (SEM). The instrument also provided deposit elemental results using energy-dispersive x-ray (EDX). SEM micrographs of the same four segments shown in Figure 9 were taken to allow comparison, and are given in Figure 10. These images were produced by the collection of secondary electrons, and are a useful way of examining surface topography. The milled surface is visible on either side of the flow channel, providing a frame of reference (flow direction for these images was vertical). For SEM images, steep surfaces result in higher angle of incidence with the beam and thus a brighter surface. This is seen on the sloping sides of the tube sections. Dark spots on the blank (a) and inlet (b) sections may indicate contamination from the test section handling pieces although, if handling procedures were uniform, similar spots would be expected for the outlet (d). Minor contamination was almost inevitable, although care was taken to minimize it. It is also possible that the large dark feature near the top of image (b) is the onset of deposit formation. The noticeably darker color of for the middle segment (c) indicates the difference in surface morphology due to deposit. Micrographs at higher magnification (not shown here) revealed a relatively smooth and uniform surface of the middle segment (c). No shedding of deposit was evident.

The elemental composition of the four segments, determined by EDX spectroscopy, is given in Figure 11. A sharp decrease in copper content with an accompanying increase in carbon indicates coke formation in the middle segment. Contamination on the blank segment causes an increase in carbon signal. Oxygen content for all segments is likely due to adsorption from the atmosphere. A peculiar result of the analysis is the 0% carbon content in the outlet segment. Given the relatively high temperature fuel exposure to this surface for extended duration, at least a small carbon signal might be expected. Further examination of axial distribution of carbon content is necessary to explore this result.

from the light source (flow direction for these images was horizontal). The lengthwise grooves visible in the blank segment are characteristic of the manufacturing process for extruded copper tubes and should not be mistaken as a deposition feature, although they are likely to influence heat transfer and deposit buildup. The inlet segment is discolored, which may indicate the onset of deposit buildup. The presence of coke formation on the middle segment is obvious as a gray-black, matte buildup. The layer of deposit appeared uniform in general, with noticeable topography in areas of thicker deposition. In areas where the deposit appeared thinner, the orange-brown copper surface was visible underneath. The surface also featured an almost plate-like structure, with small fissures forming in certain areas. The outlet segment is discolored but does not show visible coking.

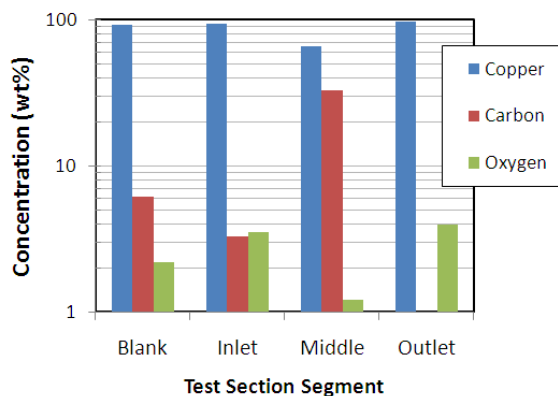


Figure 11. Elemental Composition of tube segments determined by SEM/EDX. Thermally stressed tube sections were analyzed for composition. The carbon content of the middle section shows evidence of coking. Oxygen content of all segments is likely due to adsorption. 2σ uncertainty for middle segment Cu and C concentration based on four measurements is ± 6 wt%

C. LECO Carbon Deposition Analysis

In addition to qualitative inspection of test section surfaces, four 1-in. tube segments were taken from each test section (labeled A, B, C, and D in Figure 8) and used for carbon deposition measurements. Two unused test sections were handled identically, segmented, and provided for comparative purpose. A LECO RC-412 Carbon Determinator oxidized the segments in a high temperature furnace under controlled oxidizer flow and related the time-integrated concentration of the resulting products to total carbon. This has become a somewhat standard way of reporting carbon coking in hydrocarbon fuel thermal stability research.^{8,9}

Carbon burn-off test results from five long-duration, high-wall temperature tests are presented in Figure 12. Deposition results (D) have been normalized by the maximum measured deposition for all pieces (D_{\max}), which occurred in segment C of Run 132. From these results, there appears to be no identifiable correlation between tube axial location and deposit. For example, according to Figure 8, one might expect higher levels of deposition for segments B and C, since they were in direct contact with the heater block and exposed to the greatest temperature. But this pattern is only seen for Run 132. It is unlikely that the differences in measured deposit are due to misalignment between the heater block and the tube, causing large temperature differences and variation in deposited carbon. The variability in deposit results for the blank tube segments may indicate uncertainties (associated with the test handling and/or measurement procedure. However, it is unlikely that differences in measured deposition, e.g. see Run 132, are purely random in nature (especially given the visible contrast between inlet, middle, and outlet segments as seen in Figure 9). Given the low sample size (four samples per run), the discrepancies in the deposition results are likely a combination of random errors and real phenomena. In this case, the blank section results were used to obtain a standard deviation which was used in the

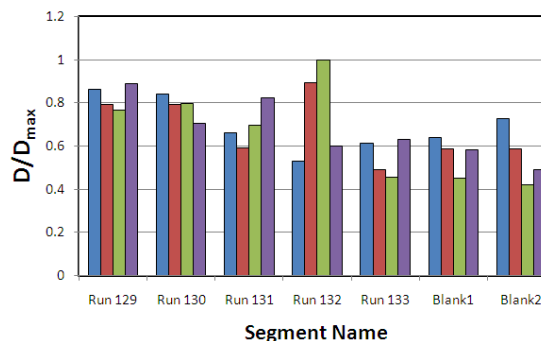


Figure 12. Carbon deposition normalized by maximum deposition measured. A LECO RC-412 was used for the carbon burn-off results shown here. Test segments were 1-in. long. Two blank sections, not exposed to fuel, were taken for comparison.

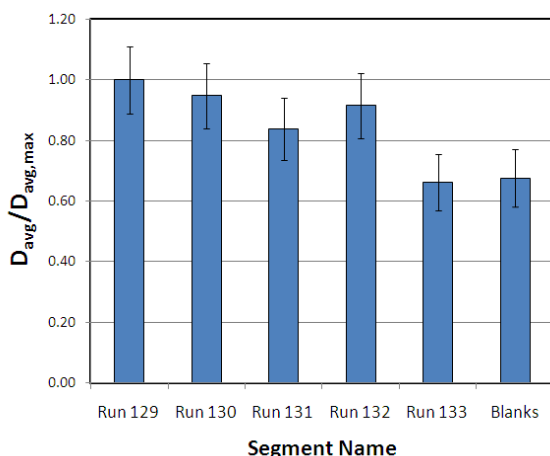


Figure 13. Normalized, average carbon deposition results. Tube-averaged deposition measurements showing tube-deposit formation trends for high temperature thermal stressing tests of RP-2. Combined uncertainty was estimated from 1σ of the eight blank segments and the stated measurement uncertainty.

too short to produce deposit formation, at least for cases when previously unstressed fuel is used. Comparing Runs 129 and 132, it appears that bulk temperature has little influence on solid deposit formation at the wall. Even with the large bulk temperature difference between the two runs, the measured deposition is very close. Although higher

bulk temperature leads to increased heat transfer in the thermal boundary layer, pyrolytic decomposition reactions and deposit formation on surfaces are wall effects influenced by temperature at or near the wall, and are not likely to be sensitive to bulk temperature variation. To summarize the deposit results: longer run times are needed to produce carbon deposits which can be resolved from the blank segments; the variation in carbon deposit for a given run is likely a combination of random experimental error and physical phenomena; preheating the fuel does not appear to play a dominant role in deposition, but further testing will explore this effect; reusing thermally stressed fuel is likely to influence deposit formation. Finally, although these results present some useful information, repeated tests at specific conditions will result in a statistical population, allowing more meaningful comparisons of deposition data.

Table 1. Conditions for longer-duration thermal stressing tests

Run	Preheater %	T _{m,o} °F (K)	Fuel Condition (pre-test)	Avg. Heat Flux Btu/in ² s (MW/m ²)	Duration min.	Velocity ft/s (m/s)
129	5	191 (362)	recycled	6.13 (10.0)	36	52 (16)
130	50	292 (417)	recycled+1 run	6.81 (11.1)	37	54 (16)
131	75	430 (494)	fresh	6.72 (11.0)	33	60 (18)
132	75	431 (495)	fresh+1 run	7.17 (11.7)	33	61 (19)
133	75	435 (497)	fresh	7.30 (11.9)	35	61 (19)

IV. Summary and Conclusions

AFRL's High Heat Flux Facility has been demonstrated as a test rig capable of simulating the extreme environment found in regenerative cooling channels. Thermal stability testing of RP-2 in a conductively-heated rig was performed with varying wall temperature, bulk fuel temperature, test duration, and test section flow rate. Average convective heat transfer coefficient was measured for several short-duration tests, and nondimensionalized heat transfer (Nusselt number) was compared with an existing empirical correlation for RP-1. Good agreement with the correlation was seen when the experimental data was corrected for inner (wetted) wall temperature, which was shown to vary substantially around the circumference of the tube wall. This circumferential variation in wall temperature is characteristic of asymmetric heat transfer experiments, and will be considered when reporting wall coking temperature limits. The effects of mass flow rate, bulk inlet temperature, and wall temperature on heat transfer were shown to be consistent with expected trends. To improve the fidelity of heat transfer correlations for rocket kerosenes, accurate thermophysical property (e.g. absolute viscosity, extremely temperature-dependent) information at high temperature and pressure is needed. This need is currently being addressed under Air Force-directed programs.

Longer-duration tests at very high wall temperatures were intended to explore the maximum allowable wetted wall temperature (coking limit) of RP-2. For these tests, evidence of carbon deposit formation was witnessed qualitatively with optical and scanning electron microscopes, and SEM/EDX elemental analysis showed carbon coverage on the inner surface of the heated portion of the tube, but very little on the tube portions outside the heated region. Carbon deposit formation was measured with a LECO carbon determinator. These tests indicate that high bulk fuel temperature may not play a dominant role in deposition, but further testing is required to explore this effect. The measured deposition for five high-wall temperature tests was not significantly greater than that of a blank test section, and therefore experimental modifications (e.g. lower velocity, longer duration, and higher wall temperature) are required to accurately quantify the conditions and rates at which deposit formation becomes unacceptable. The variation in deposit results also reflects random experimental and instrument uncertainties, and therefore repeated tests at a given condition are necessary before making conclusions regarding wetted wall temperature limits for deposit formation rates.

Acknowledgements

The author would like to thank Dr. Tim Edwards and Mr. Dave Brooks (AFRL/RZTG) for useful discussion and LECO carbon deposition measurements; Dr. Simon Lyu (Advatech Pacific) for his CFD modeling effort; and Ms. Marietta Fernandez and Mr. Wesley Alleman (AFRL/RZSM) for their help with SEM/EDX analyses. The ongoing insight and support of Dr. Ingrid Wysong and Dr. Steve Danczyk (AFRL/RZSA), and Mr. Ron Bates (CPIAC) is appreciated. The dedication and efforts of Mr. Dave Hill, Mr. Earl Thomas, Mr. Randy Harvey, and Mr. Paul Rue (ERC, Inc.); Mr. Mark Pilgram and Mr. Todd Newkirk (JACOBS Engineering); and Mr. Alan Baxter (AFRL/RZSO) are appreciated.

References

- ¹ Maas, E., Irvine, S., Bates, R., and Auyeung, T., "A High Heat Flux Facility Design for Testing of Advanced Hydrocarbon Fuel Thermal Stability," (AIAA) 2005-363 at *43rd AIAA Aerospace Sciences Meeting and Exhibit*, Reno, NV, 2005.
- ² Stiegemeier, B., Meyer, M.L., and Taghavi, R., "A Thermal Stability and Heat Transfer Investigation of Five Hydrocarbon Fuels: JP-7, JP-8, JP-8+100, JP-10, and RP-1," (AIAA) 2002-3873 at *38th AIAA/ASME/SAE/ASEE Joint Propulsion Conference*, Indianapolis, IN, 2002.
- ³ Billingsley, M.C., Lyu, H.Y., and Bates, R.W., "Experimental and Numerical Investigations of RP-2 Under High Heat Fluxes," at *54th JANNAF/3rd Liquid Propulsion Subcommittee Meeting Joint Meeting*, Denver, CO, 2007.
- ⁴ Liang, K., Yang, B., and Zhang, Z., "Investigation of Heat Transfer and Coking Characteristics of Hydrocarbon Fuels," *Journal of Propulsion and Power*, Vol.14, No.5, 1998. pp. 789-796.
- ⁵ Stiegemeier, B.R., Meyer, M.L., and Driscoll, E., "RP-1 Thermal Stability and Copper Based Materials Compatibility Study," at *JANNAF 1st Liquid Propulsion Subcommittee Meeting*, Las Vegas, NV, 2004.
- ⁶ Coleman, M.M., Selvaraj, L., Sobkowiak, M., and Yoon, E., "Potential Stabilizers for Jet Fuels Subjected to Thermal Stress Above 400°C," *Energy and Fuels*, Vol.6, No.5, 1992. pp. 535-539.
- ⁷ Andersen, P.C., and Bruno, T.J., "Thermal Decomposition Kinetics of RP-1 Rocket Propellant," *Ind. Eng. Chem. Res.*, Vol.44, No.6, 2005. pp. 1670-1676.
- ⁸ Giovanetti, A.J., Spadaccini, L.J., and Szetela, E.J., "Deposit Formation and Heat-Transfer Characteristics of Hydrocarbon Rocket Fuels," *Journal of Spacecraft*, Vol.22, No.5, 1985. pp. 574-580.
- ⁹ Edwards, T., DeWitt, M.J., Shafer, L., Brooks, D., Huang, H., Bagley, S.P., Ona, J.O., and Wornat, M.J., "Fuel Composition Influence on Deposition in Endothermic Fuels," (AIAA 2006-7973) at *14th AIAA/AHI Space Planes and Hypersonic Systems and Technologies Conference*, Canberra, Australia, 2006.